ELSEVIER

Contents lists available at ScienceDirect

Fuel

journal homepage: www.elsevier.com/locate/fuel



Full Length Article

Variables governing the initial stages of the synergisms of ultrasonic treatment of biochar in water with dissolved CO₂



Baharak Sajjadi^{a,*}, Wei-Yin Chen^a, Adedapo Adeniyi^a, Daniell L. Mattern^b, Joel Mobley^c, Chin-Pao Huang^d, Ruimei Fan^d

- ^a Department of Chemical Engineering, University of Mississippi, University, MS 38677, United States
- ^b Department of Chemistry and Biochemistry, University of Mississippi, University, MS 38677, United States
- ^c Department of Physics and National Center for Physical Acoustics, University of Mississippi, University, MS 38677, United States
- ^d Department of Civil and Environmental Engineering, University of Delaware, Newark, DE 19716, United States

ARTICLE INFO

Keywords: Biochar Heating values Gasification pretreatment Sonochemistry

ABSTRACT

The objectives of a series of our researches are to determine the feasibility of applying ultrasonic pretreatment prior to biochar gasification. As per the initial results, the heating value (HV) of biochar significantly increased after acoustic treatment in water with dissolved CO2 (AIChE Journal, 2014;60:1054-1065). Accordingly, emphasis of the current work is placed on the parameters governing the HV of biochar in the early stage of the treatment. Switchgrass and miscanthus biochars were treated under different conditions. The reactant ratio, biochar:water:CO2, exhibited profound impacts on the synergism. The highest (but not yet systematically optimized) ratio of HV increase (or HV Gain, HG) to ultrasound energy supplied (ES) takes place when biochar-towater ratio, or BC:W, equals 0.06 g/ml. The observed HG/ES is about 10, suggesting that the energy consumption is only a fraction of the acoustic energy supplied. Miscanthus biochar's HV increases by up to 4.6% after treatment at 5% amplitude for 135 s (HG = 33 cal/g). For the same run, miscanthus biochar's H content increased by 42.7%. Changes in HV can be mediated by mineral leaching, C or H fixation, or O content loss. Mineral leaching is influenced by pH and CO2 concentration. CO2 and water are the sole contributors to C and H gains, respectively. CO2 concentration in the solution during the treatment is also affected by mass transfer limitations, ultrasound power, and design of the three-phase reactor. Increasing the BC:W ratio initially enhances the cavitation nuclei on the fluid/solid surface, and therefore sonolysis. The subsequent decrease in HV with increasing BC:W may be due to the limitation in ultrasound penetration and H supply from water. Carbon and hydrogen fixation may be connected to the formation of H2, CO, formic acid, formaldehyde, and associated radicals during sonolysis of aqueous CO2

1. Introduction

Biochar (BC) in water saturated with CO_2 undergoes several synergistic chemical and physical processes under ultrasonic and/or light irradiations: [1] exfoliation of the graphite and graphitic oxide clusters, reductive fixation of CO_2 through carboxylation, hydrogenation by water, and leaching of minerals. These processes, combined with water splitting, result in increased carbon and hydrogen content, higher internal surface area, lowered mineral content, and higher heating value of the biochar. All these synergisms take place simultaneously in a single-stage reactor containing BC in H_2O saturated with CO_2 at $65\,^{\circ}C$ and under 1 atm of CO_2 in the headspace. The temperature of the BC/ H_2O/CO_2 system rises from ambient temperature to $65\,^{\circ}C$ during the

treatments mainly due to heat generated from the ultrasound horn and Xe lamp. Ultrasound irradiation of BC in water can also increase the internal micro, meso and macropore surface area and pore size in BC and in the presence of CO_2 dissolved in water; an appreciable amount of CO_2 is fixed on BC during synergisms of acoustic and photochemical treatments, hence this approach has been considered a carbon activation process [2]. These discoveries lead to several transformative technological concepts for producing advanced sorbents for CO_2 capture [2] and adsorption of heavy metal ions in wastewater [3]. Conventional carbon activation requires heating at temperatures greater than $700\,^{\circ}$ C for over 3 h, while the synergisms of acoustic and photochemical treatments have been observed at essentially ambient conditions. Thus, carbon activation by acoustic and photochemical

E-mail address: bsajjadi@olemiss.edu (B. Sajjadi).

^{*} Corresponding author.

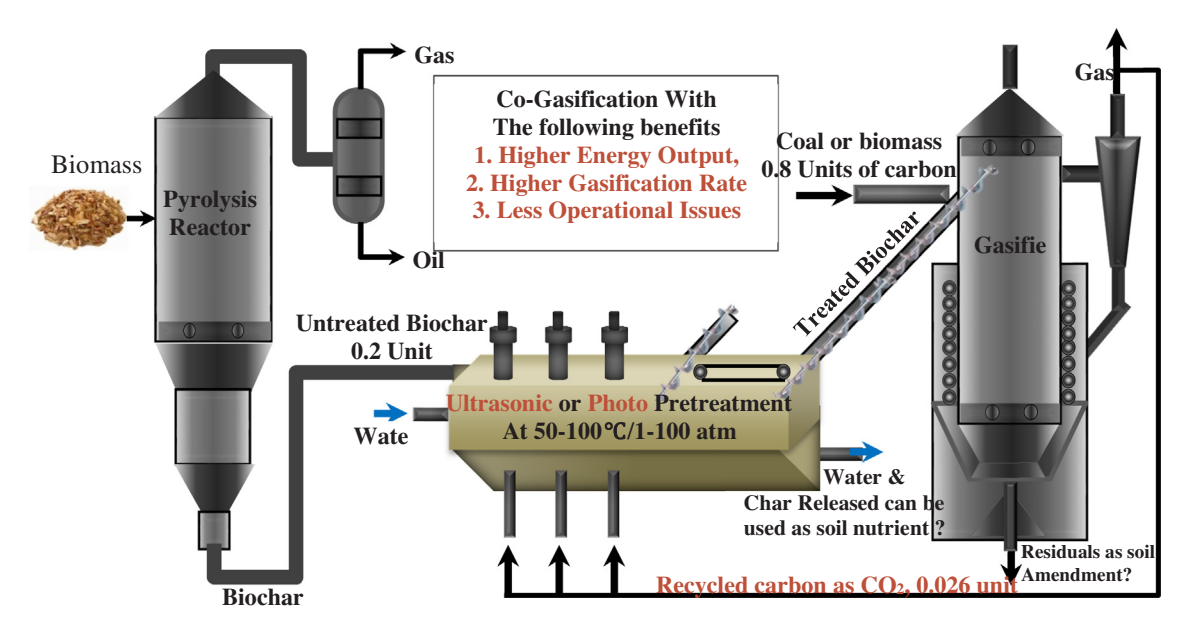


Fig. 1. The ultrasonic or photo pretreatment of biochar with CO₂ and water in a co-gasification process with two fuels sources induces multiple synergisms in a single step of operation.

treatments is an energy efficient and cost effective technique for the production of activated carbon.

The observed increases in BC's heating value after the treatment are attributed to addition of hydrogen and carbon elements from H2O and CO₂, respectively, and by mineral leaching [1]. Changes in oxygen content do not appear to be significant. Consequently, to the extent that these treatments fix the carbon of CO2 to solid fuel, they create a cradleto-cradle carbon chemical looping. Specifically, it appears plausible to consider acoustic treatment of BC in H₂O/CO₂ as a pretreatment unit operation prior to its gasification, (see Fig. 1). Gasification is a power generation process. Increasing the heating value of the biochar (or charcoal) subsequently increases the efficiency of the gasification process. This increment is achieved through two mechanisms, i) Increasing the carbon and hydrogen contents of the biochar structure (manipulation of the structure), ii) removal of ash content from the biochar structure. A series of our studies have shown that ultrasound irradiation of the biochar structure in water in the presence of dissolved CO2 can simultaneously impose both mechanisms to the biochar. Ultrasound also increases the porosity of biochar. It is well-known that the porosity of carbonaceous structures has a direct effect on the rate and efficiency of gasification [4]. Increasing the heating value of biochar not only increases the efficiency of the gasification, but also reduces the need to use very high temperatures. Moreover, CO2 as one of the main products of gasification is one of the inputs of the ultrasono-pretreatment unit since the process needs dissolved CO2. Therefore, the total output of CO₂ is reduced in such a process. On the other side, steam is one of the gasifying agents. Biochar sonicated in water has enough moisture to supply the steam required for gasification; it is not necessary to expend energy to dry the treated biochar. Therefore, mixing a small portion of the treated biochar with raw biochar can significantly improve the gasification rate and efficiency. In recent years, the integrated-gasification combined cycle (IGCC) has emerged as a versatile and efficient technology for converting solid fuels to power, heat and chemicals [5]. Nevertheless, it remains highly desirable to further improve its efficiency. Advanced concepts for the energy-intensive pre-combustion CO₂ capture operation have gained increasing attention. Moreover, the improvement in IGCC's thermal efficiency is another active research topic. The single-stage, acoustic pretreatment, as depicted in Fig. 1, seems to be capable of significantly improving both the energy efficiency and CO2 capture for advanced IGCC [1]. It certainly warrants a systematic investigation.

The interactions among the biomass origin, pyrolysis conditions, acoustic pretreatment procedure, reactor design, and treatment conditions comprise a complex network of variables that have profound influences on the properties of the treated BC. The objective of the current work is to elucidate the major variables governing the gain in heating value and carbon and hydrogen uptakes of BC in the early stage (up to less than 3 min) of the acoustic treatment of the BC in $\rm H_2O$ with dissolved $\rm CO_2$. We are particularly interested in determining if the acoustic energy consumption is sufficiently low in achieving these synergisms.

Two BCs were selected based on the hypothesis that BCs with high surface alkalinity favor the previously observed synergisms of chemical reductions of BC under acoustic treatment. Specifically, switchgrass and miscanthus pyrolyzed at 550 and 700 °C, respectively, were chosen for comparison. It is known that biochars contain redox-active moieties that are dominantly either electron-accepting or electron-donating depending on the pyrolysis temperature of production of such chars [6]. The high alkalinity of the carbon surface favors adsorption of protons and Lewis acids in aqueous solutions [7,8]. Miscanthus BC and switchgrass BC produced above 400 °C have a pH ~10 [9], which is considered high among the BCs [10]. Moreover, acidic organic functional groups, including carboxylic acids and phenols, are removed from the BC surface during the heat treatment of biomass [11-14]. Therefore, carbons produced from the high-temperature process usually have higher alkalinity [11]. Comparison of the behaviors of miscanthus and switchgrass biochars produced at 700 and 550 °C should provide additional support for the hydrogen and carbon fixation on biochar during acoustic treatment.

2. Experiments

2.1. Biomass preparation

Switchgrass and miscanthus, denoted as SG and Misc, respectively, were obtained from the Idaho National Laboratory (INL). They were ground and sieved to fine particles of size ranges 75–106 μm and 75–250 μm before drying under vacuum overnight at 60 °C prior to pyrolysis. The dried biomass was left to naturally cool to a temperature below 40 °C under vacuum before being weighed and immediately transferred to the pyrolyzer for pyrolysis to reduce moisture pickup by the sample. The grinding was done using the IKA MF10 basic continuous feed grinder and sieving was carried out using the Gilson SS-

15D 8 in sieve shaker with digital timer set at 40 min. The sieved biomass consisted of more particles in the size range of $212\text{--}250\,\mu m$ than in the $75\text{--}212\,\mu m$ range. Thus, grinding of biomass with this feed grinder to the particle size range of $75\text{--}106\,\mu m$ was a time-consuming operation as it required repeated grinding of the same batch of sample. This limitation prompted the choice to increase the size range to $75\text{--}250\,\mu m$ for later experiments.

2.2. Pyrolysis setup and conditions

Biochars were produced from two different pyrolysis reactors. The switchgrass BC was produced at 550 °C using an electrically heated tube furnace and the miscanthus BC was produced at 700 °C using a muffle furnace. Two different pyrolysis temperatures were applied to increase the biochar's surface alkalinity in a Lewis sense for adsorption of Lewis acids. Switchgrass BC has naturally higher alkalinity compared with Miscanthus BC. Therefore, a higher temperature was used to increase the alkalinity of Miscanthus BC. Comparison of pH value of biochar mixed with water demonstrated the pH values of around 11.5 and 10.1 for switchgrass and Miscanthus biochars pyrolyzed at 550 °C and 700 °C, respectively. The biochars were denoted SG 550 and Misc 700 in terms of material and production temperature. Raw Misc 700-a and Misc 700-b denotes miscanthus BCs of particle size ranges of 75–106 μm and 75–250 μm , respectively.

2.2.1. Tube furnace pyrolysis system

The switchgrass BC was produced in an alumina tube vertically placed in a tube furnace using the same layout used previously [1]. Six grams of dried switchgrass wrapped in a 350 mesh stainless steel cloth was pyrolyzed in the alumina tube at a rate of 5 °C/min to 550 °C. The sample was held for 10 min at the peak temperature before being ramped down at the same rate to room temperature. Volatiles were swept downstream by ultra-high purity He at a 400 ml/min flowrate and collected by a filter. The He carrier gas passed through another tube furnace containing Cu-turnings before entering the pyrolysis reactor. Cu-turnings remove the trace oxidants in He gas at 500 °C before He enters the pyrolysis reactor, and therefore minimize biochar oxidation during pyrolysis. Copper oxides were periodically reduced to regenerated Cu at 500 °C by passing CO through the reactor. This apparatus produced BC free of contact with oxidants but yielded only 2 g of biochar in 2 days from each pyrolysis experiment. This limitation rendered it necessary to find an alternative method to produce biochar at a higher rate for the subsequent treatments and characterizations.

2.2.2. Muffle furnace pyrolysis system

A porcelain ceramic wide-form crucible of capacity 250 ml, diameter 102 mm and height 60 mm, was filled with the dried miscanthus biomass and covered with a lid. The covered crucible was then placed in a muffle furnace with a 20 °C/min heating ramp to a final temperature of 700 °C at ambient pressure and limited oxygen environment. The temperature 700 °C was held at for 2 h before switching off the furnace and allowing it to naturally cool to room temperature. In order to limit the accessibility of O_2 to the biomass, we used two different strategies simultaneously. I) Very well-made crucibles with covers were used. The crucibles were filled with biomass to their maximum capacity to limit the space for any extra gas. II) 8 crucibles

(all full of a unique biomass) were simultaneously placed inside the muffle furnace to not only reduce the volume of any extra gas (air) inside the muffle furnace, but also to increase the volume of bio-gas and bio-oil generation; so that the output rate of these products did not allow any gas to come in. Yet, a very thin vanilla-colored layer of ash was found at the top of the BC formed near the edge of the crucible after each pyrolysis experiment unlike in the tube furnace pyrolysis. This could be attributed to its, albeit limited, contact with oxygen. In order to ensure reproducibility, this very small quantity of ash was mixed thoroughly with the biochar sublayer before storage for subsequent characterization and experiments.

2.3. Ultrasound treatments

In our previous study, BC in $\rm H_2O$ saturated with $\rm CO_2$ in a glass flask was treated by a laboratory ultrasound cleaner of 90 W at 38.5 to 40.5 kHz [1]. A significant fraction of acoustic energy dissipated in the water bath before it entered the glass flask. Moreover, the acoustic energy consumed by the solution could not be measured. To maximize the utilization of acoustic energy, the current study adopts a new sonicator, QSonica Q700, that allows direct insertion of its ultrasound probe of 1.27 cm diameter into the liquid solution. It generates ultrasound at 20 kHz and power up to 700 W. A digital display on the controller showed the energy emitted into the solution.

2.3.1. Ultrasonic treatments of switchgrass biochar

Before the acoustic treatment, pure CO_2 was bubbled through a solution containing 3 g of BC and 250 ml of de-ionized (DI) water in a 400 ml Pyrex beaker at a 50 ml/min flowrate for 30 min. To investigate the effects of CO_2 , we conducted two kinds of treatments of switchgrass BC. The first kind was performed in a beaker open to ambient air, and the second kind was in a beaker inside a Labconco glovebox purged and filled with CO_2 at 1 atm.

After the treatment, filtration was performed using a Whatman cellulose filter paper (CFP 4) with pore size of about 20–25 μm , and with ultra-pure (type 1) DI water (18.2 M Ω .cm) from a Direct-Q* 3UV lab water system. The filter paper containing the wet biochar was dried at 60 °C overnight in a vacuum oven. Weights of the dried BC were recorded before and after the treatment. The pH of the DI water was measured in three different steps: after mixing with BC, after CO₂ bubbling, and after ultrasound treatment.

2.3.1.1. Treatments open to air. The BC-water-CO₂ mixture in a Pyrex beaker, open to the atmosphere, was sonicated at 100% amplitude for 11 or 22 s with the probe vertically inserted about 1.27 cm into the center of the solution. Weights of BC before and after treatment were recorded; weight change during treatment is pivotal to the estimations of BC's mineral loss, and gain and loss of organics.

2.3.1.2. Treatment in glove-box. For the study of the effects of CO_2 in the headspace, the beaker containing the 3 g BC/250 ml H_2O /saturated CO_2 was taken into the glovebox immediately after CO_2 bubbling. The glovebox was then purged with pure CO_2 and evacuated three consecutive times. The sonication was conducted under 1 atm CO_2 for 11 or 22 s followed by filtration and drying.

Table 1 shows the treatment conditions of switchgrass including the

Table 1
Comparison of miscanthus and switchgrass biomass proximate, ultimate and calorimetry.

Biomass	Proximate, dr	y basis		Ultimate, dry b	asis	Calorimetry				
	Volatile, %	Ash, %	Fixed Carbon,%	Hydrogen, %	Carbon, %	Nitrogen, %	Oxygen, %	Sulfur, %	HHV, kcal/g	LHV, kcal/g
Switchgrass Miscanthus	80.2 85.53	4.2 1.4	15.6 13.06	5.7 5.85	47.2 50.64	0.5 0.21	N.D. 41.88	N.D. 0.01	4.487 4.718	3.749 3.929

^{*} Idaho National Laboratory Data.

Table 2
Treatment of switchgrass biochar pyrolyzed in tube furnace at 550 °C: treatment conditions, changes in biochar weight, pH, mineral content and organics, heating value, heating value gain by biochar.

	Raw BC	SG 550-1	SG 550-2	SG 550-3 ^a	SG 550-4 ^a
Mass of BC used in the sonication, g, (dry)		3	3	3	3
pH of de-ionized water		5.68	5.77	5.64	5.85
Water volume used, mL		250	250	250	250
pH of $H_2O + BC$		11.53	11.55	11.54	11.57
pH of $H_2O + BC + CO_2$		6.08	6.04	6.10	6.13
Amplitude of sonication, %		100	100	100	100
CO ₂ in headspace		400 ppm	400 ppm	100%	100%
Sonication time, s		11	22	11	22
U.S. energy supplied, kcal/g		0.08	0.16	0.08	0.16
Maximum temperature, °C		21	23	22	23
pH of filtrate		6.78	6.79	6.53	6.66
Weight change, %, (dry)		-2.08	-2.66	-1.99	-2.39
Ash content analysis, %	23.00	21.46	21.06	21.50	21.04
Percentage change in sample's mineral weight		-8.64	-10.87	-8.38	-10.71
Organic content (by difference), %	77.00	78.54	78.94	78.50	78.96
Percentage change in sample's organic weight		-0.12	-0.21	-0.08	0.09
Heating value, kcal/g, (dry)	5.71	6.00	6.08	6.01	5.97
Change in Heating Value, kcal/g, (dry)		0.29	0.37	0.30	0.26
Percentage Increase in Heating Value		5.08	6.48	5.25	4.55

^a Done in the glovebox under 1 atm of CO₂.

changes in weight, pH, mineral content and organics during treatment. Mineral leaching, organic leaching and organics gain can take place simultaneously during the treatment [1]. Thus, weight change in combination with the change in mineral content of the BC during treatment allow us to estimate the losses (or gains) in organics and mineral content for all treated samples. The percentage loss/gain of the minerals and organics compared to the raw biochar are included in Table 2.

2.3.2. Ultrasonic treatments of miscanthus biochar

To elucidate the major treatment process variables that affect the BC's properties such as its heating value, carbon and hydrogen fixation, and mineral leaching, we designed two sequential groups of treatments for miscanthus BC. Particular attention was placed on ultrasound power, BC/H $_2$ O ratio, and CO $_2$ concentrations of the solution and above the solution.

2.3.2.1. Effects of CO_2 in the solution and sonication power. The aim of this group of experiments was to investigate the effects of CO_2 in the BC/H₂O solution and ultrasound power. In our previous work, treatment without CO_2 bubbling showed a certain degree of carbon fixation, and CO_2 trapped in water was suspected to play a role [1]. In run Misc 700-1, He gas (rather than CO_2) was used to purge reactive gases, such as CO_2 , out of the 250 ml DI water for 30 min, followed by the addition of 3 g BC and an additional 30 min purging with He. The solution was then filtered, and the BC and the filtrate were analyzed without acoustic irradiation.

In the other four treatments in this set of experiments, $3\,\mathrm{g}$ BC/250 ml H₂O underwent preliminary CO₂ bubbling at $50\,\mathrm{ml/min}$ for $30\,\mathrm{min}$. One of the samples, Misc 700-2, was filtered after CO₂ bubbling without sonication, while the three others underwent varying ultrasonic irradiations. Misc 700-3 and Misc 700-5 were sonicated using the 100% amplitude of the instrument, but for different times of $35\,\mathrm{and}$ 22 s, respectively. Misc 700-4 was sonicated using 5% of the maximum amplitude of the instrument for $150\,\mathrm{s}$. Total ultrasound energy expenditure for Misc 700-4 and Misc 700-5 was maintained at the same value of $\sim 2.050\,\mathrm{kJ}$ ($0.160\,\mathrm{kcal/g}$), but for Misc 700-3 the energy was $\sim 3.100\,\mathrm{kJ}$ ($0.253\,\mathrm{kcal/g}$).

2.3.2.2. Effects of CO_2 in the head space and BC/H_2O ratio. During the course of this study, we were increasingly concerned about the effects of the stoichiometric ratio of the three reactants, $BC:H_2O:CO_2$. To

investigate the effect of the BC:H $_2$ O ratio, Misc 700-6 followed the same procedure as Misc 700-4 except that 15 g (rather than 3 g) of BC was used. Misc 700-7 followed the same procedure as Misc 700-6 except that a gas mixture containing 15% CO $_2$ balanced with He was blown into the headspace of the solution during ultrasound treatment. Supplying CO $_2$ into the headspace not only minimizes CO $_2$ escape from the saturated solution, but also replenishes the CO $_2$ in the solution due to the consumption by reaction. Misc 700-8 followed the same procedure as run Misc 700-7 except that 80 g BC in 400 ml of H $_2$ O was used and a gas mixture containing 7% CO $_2$ balanced with He was blown into the headspace of the solution during ultrasound treatment. It is worth mentioning that 400 ml of H $_2$ O is the minimal quantity of water to fully wet the 80 g BC, but little ultrasound-induced mixing was observed.

While runs Misc 700-1 to Misc 700-7 were done with BCs of particle size 75–106 μm , runs Misc 700-9 to Misc 700-12 were done with BCs of particle size 75–250 μm . Misc 700-9 and Misc 700-10 followed the same procedure as Misc 700-7 except that 30 g of BC was used in both runs and a gas mixture containing 15% CO $_2$ for Misc 700-9 and 7% CO $_2$ for Misc 700-10, balanced with He, was blown into the headspace. Misc 700-11 and Misc 700-12 followed the same procedures as Misc 700-9 and Misc 700-10, respectively, except that 40 g of BC and 100% amplitude of the instrument was used. Analyses for Misc 700-11 were done in duplicate with the standard deviations reported.

2.4. Characterizations

2.4.1. Sorptometry

Surface area measurements and pore volume distribution were done with the Quantachrome NOVA 1200 gas sorption analyzer. Degassing of all samples was done for 3 h at 300 °C before analysis. The internal surface area, pore volume and size distribution of meso and macropores were measured with $\rm N_2$ at -196.15 °C and those of micropores were conducted with $\rm CO_2$ at 0 °C. In addition, surface area of macro and mesopores was estimated by the Brunauer-Emmett-Teller (BET), equation and surface area of micropores was estimated by the Dubinin-Radushkevich (DR) equation. Pore size distribution was analyzed by using the DFT (Density Functional Theory) method. Equilibrium pressure tolerance was set at 0.10 mmHg, equilibrium time tolerance 240 s, and maximum equilibration time of 600 s. More details about these analyses can be found in an earlier publication of ours [15].

2.4.2. pH, elemental analysis, heating value, ash analysis

All pH measurements were performed with an Oakton pH 700 Benchtop Meter. Analyses of C, H, O, N, S and selected metal elements in biochar and aqueous solutions were conducted at Huffman Hazen Laboratories. Heating value was calculated by bomb calorimeter and ash percentage was determined after heating samples to 750 °C in air with a holding time of 8 h. These analyses were done at Huffman Hazen Laboratories. Ash, or mineral, content was also independently verified by using a muffle furnace in our laboratory. Heating Value Gain (HVG) was also calculated through HVG = HHV of 1g Treated BC-HHV of 1g raw BC. The initial values of organic elements (C, H, N, O and S) in both samples of miscanthus and switch grass were considered as the baseline of the calculations. However, the ash content plays an important role in determining the organic contents and can mistakenly divert or mislead the calculations. In other words, ultrasono-activation of biochar in presence of dissolved CO2 increases the mineral leaching (ash removal) from the biochar structure. If this ash removal is not considered, an increase in the percentage of C, H, N, O and S elements in the structure appears in the calculation. In this study, in order to address changes within the organic component, a WEIGHT-BASED calculation was used in which the percentage of ash removal in the total weight is considered and subtracted from the total weight to omit the effect of weight change due to ash reduction on the calculations of the organic elements (C, H, N, O and S).

3. Results and discussion

Biochars produced from switchgrass and miscanthus at pyrolysis temperatures of 550 °C and 700 °C, respectively, were tested for elucidating the effects of process parameters, namely, BC:H₂O:CO₂ ratio, concentration of CO₂ in the headspace, and acoustic energy on product characteristics, specifically, leaching of mineral matter, changes in organic content and heating value of treated chars, and pH of aqueous solutions in each step of the treatment process.

3.1. Biochar origin and pyrolytic condition

Table 1 shows the proximate, ultimate and calorimetry comparison of switchgrass and miscanthus biomasses. The miscanthus biomass contains higher volatiles, carbon, and hydrogen content, but lower fixed carbon and ash content on dry basis. Miscanthus' biochar yield (20.2 wt%, dry basis) from pyrolysis at 700 °C was notably lower than that of switchgrass biochar (31.5 wt%, dry basis) at 550 °C. This is mainly a result of the higher pyrolysis temperature adopted in the production of miscanthus biochar [16,17], and its higher volatile carbon content. The higher heating value of miscanthus over that of switchgrass biochar is a result of its lower ash content and higher hydrogen and carbon content (Table 1).

3.2. Ultrasound treatment of switchgrass biochar

Table 2 tabulates the parameters selected or measured during the treatment of switchgrass biochar, including the stoichiometric ratio of reactants (BC to water), ultrasound (US) amplitude, sonication time, ultrasound energy supplied, CO₂ concentration in the headspace, pH of the solution before and after the treatment, maximum temperature during the treatment due to the dissipation of US energy into the solution, weight change of dried BC due to the treatment, and mineral content (dry basis). Organics content is the combustible (i.e., the gasified) fraction of BC, taken as the proportion of weight lost during the measurement of minerals by muffle furnace. Table 2 also shows the gain in heating or calorific value of treated char, compared to raw char.

3.2.1. Implications of weight change

A previous study [1] suggests that mineral leaching, organics leaching, and organics gain can take place simultaneously during

acoustic treatment of BC; these three processes collectively contribute to the net change in weight of BC sample during the treatment. The weight change of BC, along with the measured mineral contents of the raw and treated BCs, allow the estimation of the net losses or gains in organics content during treatment. More importantly, in the following discussion, "mineral change" and "organics change" refer to the percentage change of the mineral and organics weights, respectively, compared to their weights in the amount of raw char needed to produce the treated sample.

The changes in overall weight and minerals and organics contents shown in Table 2 suggest that the treatment process includes a fast weight loss caused mainly by leaching of mineral matter and a small amount of change in organic compounds. The biochar samples lost an average of 2.3% of weight in less than 22 s of treatment. Ultrasound-assisted mineral leaching after 5-h treatment of sorghum biochar was more effective than mixing by a magnetic stirrer [1]. Table 2 indicates that an increase in sonication time from 11 to 22 s induces a small increase in mineral loss (i.e., "Percentage change in sample's mineral weight" in Table 2) from 8.38% to 10.71% for experiments conducted both in open-air and 1 atm CO₂ in a glovebox. This supports the conclusion that acoustic cavitation enhances mineral leaching.

3.2.2. Role of CO2

 CO_2 plays a complex role in the biochar/water/ CO_2 system. The nature of the biochar surface [12,13] as it relates to CO_2 acidity is one of the important factors. Runs SG 550-3 and SG 550-4 were conducted in a glovebox filled with CO_2 . The CO_2 in the headspace of the solution lowered the pH of the filtrate, i.e., the solution after treatment. This phenomenon is due to the reaction between water and carbon dioxide through the following reaction:

$$CO_2 + H_2O \implies O=C(OH)_2 \implies H^+ + HCO_3^-$$
 (R1

More H⁺ is formed as the amount of carbon dioxide in water increases, and hence the pH decreases. Additional H+ imposes the leachate of more metals and minerals through an ion exchange process. For example, two H+ would be able to ion exchange two monovalent species (K⁺) or one divalent species (Ca²⁺ and Mg²⁺) in the biochar [18,19]. This phenomenon not only increases the leaching of metals and mineral but also contributes to the fixation of hydrogen into the BC structure, which directly affects the heating value of biochar. In other words, the more CO2 present, the more mineral leaves and is substituted with hydrogen in the biochar structure. The effect of CO2 on mineral leaching is shown most clearly in the miscanthus BC studies below (Table 4, Misc 700-1 and Misc 700-2); however, ion exchange may play a minor role in increasing the H content of biochar. Moreover, it is known that organics in biochar can be extracted by water [20], and more acidic water, such as that saturated with CO2, is likely to retard the dissolution of biochar's acidic organics.

The effects of CO2 on the biochar's heating value offer important implications for the gasification technology we suggested at the outset of this manuscript. Acoustic treatment enhanced the heating value of treated BC by 0.26–0.37 kcal/g (4.6–6.5%) in these four experiments. The increase in heating value could be caused by mineral leaching or an increase in organic material formed on the biochar surface due to reactions between CO2 or H2O and biochar. The mineral content of these four treated biochars was about the same, i.e, ~21%, but all were less than raw biochar (23.0%). Based on the corresponding increased percentage of organic content in the treated biochars, their heating values would be expected to increase by an average of 2.2%. However, the actual average increase in heating value is about double that (5.4%). Furthermore, the net organic content of sample SG 550-4 was calculated to show an increase of 0.09%, compared to the organic content of raw char. These results are consistent with chemical bonding of biochar to C from CO₂ and/or H from H₂O during the ultrasonic treatment.

For the experiments in 1 atm CO_2 , (SG 550-3 and SG 550-4), increasing the treatment time from 11 to 22s resulted in a smaller

increase in heating value (0.30 kcal/g for 11 s vs. 0.26 kcal/g for 22 s). Based on the expected effect from mineral leaching measured for each sample, the heating value increase should have been larger for the longer sonication time. These differences are close to experimental error, but if significant, suggest that a longer sonication time degrades the chemical energy of the organic fraction of the char by unknown means. Note that longer treatment time correlates with greater heating value increases under ambient concentrations of CO2 (SG 550-1 and SG 550-2). Higher CO₂ concentrations can inhibit sonochemistry. In a review of ultrasonic pretreatment of lignocellulosic biomass for biofuel production, Bussemaker and Zhang [21] noted that the reaction severity can be enhanced by the solubility, saturation level and type of dissolved gases. Moreover, the impacts of dissolved gas depend on the ultrasound energy, and properties of the gas such as its polytropic ratio and thermal conductivity. Tri-atomic CO2 has a low polytropic ratio and has been considered inhibitive to cavitation and therefore sonochemical reactions.

Mass transfer can also play a role. In open air treatments, the acoustic cavitation causes bubbles containing CO_2 at high concentration to coalesce, grow and rise through the liquid to the surface, where they release the entrapped CO_2 to air that contains 400 ppm CO_2 [22]. This process reduces CO_2 in the solution and enhances the cavitation during the treatment, which results in slightly higher mineral leaching for runs SG 550-1 and SG 550-2 compared to SG 550-3 and SG 550-4. In a comparison of heating value increases to the amount of ultrasonic energy expended, sample SG 550-4 showed a lower ratio than that of the other samples (Fig. 2). This shows that extended ultrasonic treatment time does not improve (and may even degrade) the heating value for samples under a CO_2 atmosphere.

3.2.3. Heating value gain vs. energy supplied

Fig. 2 shows the effects of treatment time (or total ultrasound energy supplied) and CO_2 concentration in the headspace on the change in heating value of switchgrass BC. It shows that the gain in heating value is significantly higher than the ultrasound energy supplied. More importantly, it suggests that the additional investigation of the full potential of this novel treatment concept in gasification is warranted. It should be mentioned that the energy consumption is not optimized, and it can be made more efficient by several approaches. First, the design of the ultrasound horn has significant impact on the energy utilization in the treatment reactor. We are currently conducting simulations using

COMSOL's Computational Fluid Dynamics (CFD) and Acoustics modules to elucidate this hypothesis. Second, treatment parameters, such as the reactant stoichiometry, ultrasound strength, treatment time and temperature, biomass origin, and pyrolysis conditions, will have profound impact on the observed benefits. Third, a significant fraction of the ultrasound energy dissipates to the environment outside the 400 ml glass beaker during treatment. As stated in the Experimental Section, the selections of small quantities of reactants and reactor were constrained by the biochar production rate of 2 g every 2 days. The ultrasound energy efficiency should be improved for larger scale units where the dissipation is minimized.

For the experiments conducted in open air, the increasing trend of heating value gain continued to rise during the treatment time. For the experiments conducted in a glovebox under $1 \text{ atm } \text{CO}_2$, there was an optimal heating value gain during the shorter treatment time, which suggests the profound role of CO_2 in the treatment.

During the course of this study we noted the complex and sensitive roles of $CO_{2,}$ as stated above, that influence the properties of treated BC. As a consequence, the order of adding the reactants (BC and CO_{2}) into water, CO_{2} concentration in the headspace, and overall time period of the treatments can profoundly influence the reproducibility of the observations.

3.2.4. Changes in surface area and pore volume

Table 3 illustrates the changes in the micropore surface area and micropore volume of switchgrass biochars before and after treatment. CO₂ at 0 °C was used as the adsorbate and micropore surface area and micropore volume were quantified using the DR equation. All treatments notably enhanced micropore surface area and micropore volume. In a separate study, SEM images suggested that sonication cleared the volatile-filled blockages formed during pyrolysis of pinewood biochar and enhanced the micropore surface area and micropore volume [2].

Fig. 3 shows the micropore size distribution suggesting that switchgrass BC consists mainly of narrow micropores (or ultramicropores [23]) with approximate width less than $0.7\,\mathrm{nm}$. The observed increase in surface area is likely due to pore opening by ultrasound. It is also interesting to note that ultrasound notably enhanced the micropores of width $2.4\,\mathrm{\mathring{A}}$ for treatments in both air and pure CO_2 .

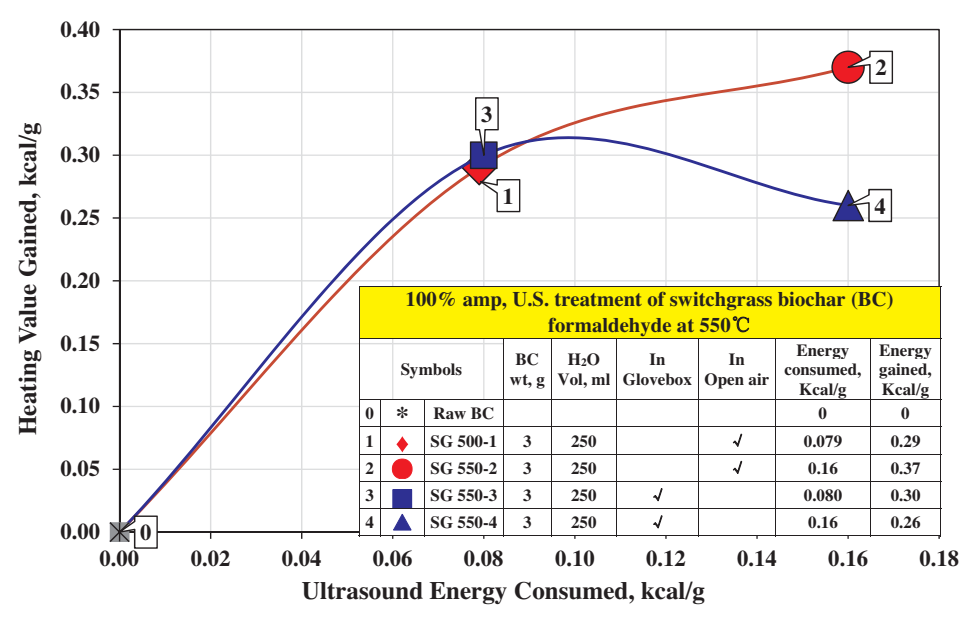


Fig. 2. Effects of treatment time (or total ultrasound energy supplied) on heating value gain of switchgrass BC.

Table 3 Changes in the surface area and pore volume of SG 550 and Misc 700 with varying treatment conditions by BET- N_2 and DR- CO_2 .

Sample	DR-CO ₂ method		BET- N_2 method	BET-N ₂ method				
	Micropore surface area, m ² /g	Pore volume, cc/g	Mesopore surface area, m ² /g	Pore volume, cc/g				
Raw SG 550	378.69	0.102	_	_				
SG 550-1	434.13	0.115	_	_				
SG 550-2	490.61	0.164	_	_				
SG 550-3	464.01	0.123	_	_				
SG 550-4	448.50	0.120	-	_				
Raw Misc 700-a	535.39	0.178	347.02	0.161				
Misc700-1	591.19	0.197	393.79	0.183				
Misc700-2	584.02	0.195	425.39	0.201				
Misc700-3	614.34	0.205	404.03	0.191				
Misc700-4	592.42	0.197	421.72	0.198				
Misc700-5	596.05	0.199	402.39	0.188				
Misc700-6	655.74	0.219	407.12	0.190				
Misc700-7	622.67	0.208	394.62	0.184				
Raw Misc 700-b	529.48	0.139	336.11	0.150				
Misc700-9	539.92	0.116	365.15	0.162				
Misc700-10	559.68	0.148	347.63	0.155				
Misc700-11*	544.92	0.128	355.50	0.159				
	(± 5.64)	(± 0.002)	(± 2.83)	(± 0.001)				
Misc700-12	551.22	0.144	361.22	0.161				

^{*} Done in duplicates with the standard deviations reported.

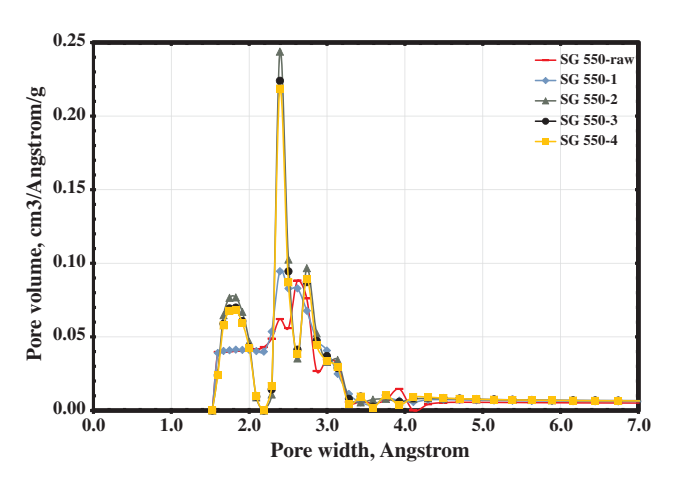


Fig. 3. . Distributions of micropore size distributions of switchgrass biochar using the nonlocal density function theory (NLDFT) model.

3.3. Ultrasound treatment of miscanthus biochar

3.3.1. Zeta potential of raw miscanthus biochar

The zeta potentials of raw miscanthus BC under different ionic strengths of sodium chloride (electrolyte) are shown in Fig. 4 with an isoelectric point pH_{IEP} (or point of zero zeta potential) around a pH of 3.5. Zeta potential is an index of the surface electric charge that a particle possesses, or acquires, when suspended in a polar medium like water [24]. A net charge is developed at the surface of BC particles due to the protonation and deprotonation of functional groups that lead to the formation of an electrical double layer in the surrounding interfacial region around each particle [25]. Fig. 4 suggests that the miscanthus BC is negatively charged at pH > pH_{IEP}, which is attributed to the increase in the basic anions on the surface of biochar [26]. This result also indicates that the basic biochar surface is subject to reactions with acidic reagents in the aqueous solution during treatments.

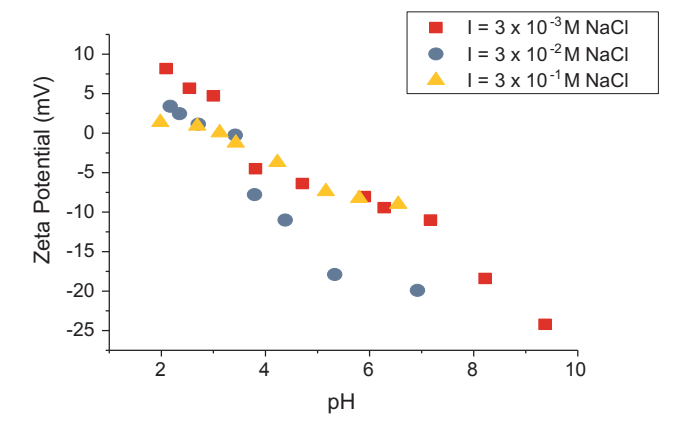


Fig. 4. . Zeta potential of raw miscanthus biochar against pH under different NaCl (electrolyte) concentrations.

3.3.2. Implications of changes in mineral and organic contents and heating value

Table 4 tabulates parameters selected or measured in different treatments of miscanthus BC, similar to those listed in Table 2 for switchgrass BC. Weight change during the treatment is a combination of mineral leaching, organics leaching and fixation of organics on biochar. Runs Misc 700-1 and Misc 700-2 were conducted without ultrasound. Misc 700-1 involved purging CO2 out of the BC/H2O solution by He bubbling. Leaching by He-purged water (Misc 700-1) removed about 0.84% and 13% of the organics and minerals, respectively. However, when CO2 was bubbled into the biochar-water mixture without sonication (Misc 700-2), about twice as much mineral matter was leached from the biochar into the leachate, with minute additional organics leaching. Comparing the changes in mineral content of Misc 700-1 with runs Misc 700-2 through Misc 700-7, and recalling the reaction between water and carbon dioxide (R1), it is apparent that CO2 enhanced mineral leaching. It also reveals that the addition of ultrasound induces additional mineral leaching. With the total ultrasound energy maintained at about the same value (0.16 kcal/g), ultrasound at its 5% amplitude (Misc 700-4) induced higher mineral leaching than at its

Fuel 235 (2019) 1131–1145

Table 4

Treatment of miscanthus biochar pyrolyzed in muffle furnace at 700 °C: treatment conditions, changes in biochar weight, pH, mineral content and organics, heating value, heating value change.

Sample ID	Raw Misc 700-a	Misc 700-1	Misc 700-2	Misc 700-3	Misc 700-4	Misc 700-5	Misc 700-6	Misc 700-7	Misc 700-8	Raw Misc 700-b	Misc 700-9	Misc 700-10	Misc 700-11*	Misc 700-1
Mass of BC used, g, (dry)		3	3	3	3	3	15	15	80		30	30	40	40
Maximum particle size, μm**	106	106	106	106	106	106	106	106	106	250	250	250	250	250
pH of H ₂ O		6.22	6.25	6.21	6.27	6.27	6.33	6.31	6.31		5.77	5.79	5.79	5.8
Water volume, mL		250	250	250	250	250	250	250	400		250	250	250	250
pH of H ₂ O + BC			10.15	10.17	10.18	10.13	10.09	10.10	9.95		10.15	10.18	$10.19 (\pm 0.01)$	10.16
Gas bubbled into BC + H ₂ O		He	CO_2		CO_2	CO_2	CO_2	CO_2						
pH of $H_2O + BC + gas$		9.9	5.9	5.82	5.92	5.89	6.32	6.33	7.38		6.72	6.74	6.98 (± 0.01)	6.96
CO2 in headspace, %		Open air	15	7		15	7	15	7					
Amplitude of sonication, %				100	5	100	5	5	5		5	5	100	100
Sonication time, s				35	150	22	135	135	129		138	138	24	24
U.S. energy supplied, kcal/g				0.253	0.166	0.160	0.033	0.033	0.006		0.016	0.016	0.012	0.012
Maximum temperature, °C				25	24	24	19	18	21		19	19	18	18
pH of filtrate following treatment		9.83	6.35	6.73	6.41	6.56	6.69	6.7	8.1		7.03	7.05	$7.51 (\pm 0.01)$	7.60
Weight change, %, (dry)		-1.6	-2.33	-3.43	-3.66	-2.86	-2.41	-2.36	-1.07		-1.97	-2.01	$-1.28 (\pm 0.00)$	-1.06
Ash content, %, (dry)	6.23	5.51	4.88	4.86	4.72	4.96	4.27	4.21	5.24	5.25	4.69	4.69	$4.74 (\pm 0.04)$	4.79
Mineral change upon treatment, (weight-adjusted) %		-13	-23.5	-24.7	-27	-22.7	-33.1	-34	-16.8		-12.4	-12.5	-10.9 (± 0.01)	-9.73
Organics contents (by difference), %	93.77	94.49	95.12	95.14	95.28	95.04	95.73	95.79	94.76	94.75	95.31	95.31	95.26 (± 0.04)	95.21
Organics change upon treatment, % (weight-adjusted)		-0.84%	-0.92%	-2.02%	-2.11%	-1.54%	-0.37%	-0.26%	0.01%		-1.39%	-1.43%	-0.75% (\pm 0.00)	-0.58%
Heating value (HV), kcal/g, (dry)	7.15	7.18	7.27	7.33	7.31	7.29	7.48	7.45	6.71	7.42	7.45	7.50	$7.44 (\pm 0.01)$	7.48
HV change upon treatment, kcal/g, (dry)		0.032	0.116	0.179	0.157	0.144	0.328	0.296	-0.441		0.033	0.077	$0.021~(~\pm~0.001)$	0.064
Change in HV, %		0.44	1.62	2.50	2.20	2.01	4.59	4.13	-6.16		0.44	1.04	$0.27~(~\pm~0.05)$	0.86
HV change/Energy Supplied				0.71	0.95	0.89	10	8.98	-73.4		2.04	4.68	1.64	5.16

^{*} Analyses done in duplicate with the standard deviations reported.

^{**} Minimum particle size = $75 \, \mu m$. ($106-250 \, \mu m$ was the major fraction for the $75-250 \, \mu m$ particles.)

Table 5
Changes in elemental Na, Si and K of miscanthus biochar with treatment.

	Na, μg/g	Si, μg/g	Κ, μg/g
Raw Misc 700-a, wt%	67	14,800	2360
Misc 700-1	63	14,300	1490
Change during treatment, %	-18%	-16%	-45%
Misc 700-2	49	13,800	1180
Change during treatment, %	- 44%	-29%	-62%
Misc 700-3	46	14,000	1170
Change during treatment, %	- 48%	-29%	-63%
Misc 700-4	57	13,800	1180
Change during treatment, %	-38%	-32%	-64%
Misc 700-5	62	14,200	1280
Change during treatment, %	-28%	-26%	-58%
Misc 700-6	39	10,800	1210
Change during treatment, %	-61%	-51%	-66%
Misc 700-7	40	11,000	1220
Change during treatment, %	-61%	-51%	-66%
Misc 700-8	59	10,200	1210
Change during treatment, %	-27%	-43%	-57%
Raw Misc 700-b, wt%	72	13,400	2560
Misc 700-9	48	12,900	1380
Change during treatment, %	- 42%	-16%	-53%
Misc 700-10	45	13,000	1410
Change during treatment, %	- 45%	-15%	-52%
Misc 700-11*	45	12,450	1485
	(± 0.71)	(± 353.6)	(± 7.07)
Change during treatment, %	- 44%	-17%	-48%
Misc 700-12	49	13,200	1680
Change during treatment, %	- 39%	-11%	-41%

^{*} Analyses done in duplicate with the standard deviations reported.

100% amplitude (Misc 700-5). An explanation is that the higher amplitude induced higher cavitation and, therefore, facilitated mass transfer of $\rm CO_2$ out the solution, diminishing the effect of $\rm CO_2$. Moreover, longer treatment time at the 100% amplitude (Misc 700-5 vs. Misc 700-3) generated somewhat higher mineral leaching, suggesting a kinetically-controlled surface reaction process.

The change in organic content of BC during treatment can include the effects of extraction of organics as well as fixation of hydrogen from $\rm H_2O$ and carbon from $\rm CO_2$; these processes are slower than mineral leaching, so their effects are more prominent at longer durations (Misc 700-6 and Misc 700-7 under sonication duration of 135 s). As per Table 6, Misc 700-6 and Misc 700-7 have had the highest H fixation, (42.7% and 38.3%), the lowest C loss (0.66% and 0.62%). However, although their extent is smaller than mineral leaching, their impact on heating value can be notable, as the highest increase in heating value was observed in these two samples. On the other hand, Wu et al. showed that water leaches both minerals and organic matter from raw biomass and biochar [20]. The leached organics produce acidic leachates that enhance further leaching of mineral matter, particularly water-insoluble inorganics.

Comparing the changes in organics content for Misc 700-1 through Misc 700-7, the effects of sonication are complex, as the ratio of biochar to water seems also to influence the extraction and fixation processes. At low BC:W ratio, the organic loss is high, suggesting the importance of extraction. When the reactant stoichiometric ratio increased from 3 g BC in 250 ml of $\rm H_2O$ (Misc 700-2 to Misc 700-5) to 15 g BC in 250 ml of H₂O (Misc 700-6 and Misc 700-7), the solution became more basic during treatment. The increased ratio of BC:H2O had profound, multiple consequences during ultrasound treatment. For example, the increased alkalinity of the solution is able to trap a higher amount of CO2 during CO2 bubbling. Hence, mineral leaching increased from an average of 24% to over 33%. This further confirms the role of CO2 and the generated H+ in removal of mineral compounds through ion exchange. On the other hand, longer sonication at lower amplitude (135 s at 5% amplitudes) has been applied to these tests. The significantly higher content of hydrogen in these two samples (2.01% and 1.95% in Misc 700-6 and Misc 700-7, respectively) suggests the fixation of hydrogen radicals generated by water splitting onto the biochar structure. However, the contribution level of either of these two phenomena (H fixation through ion exchange with H + and attachment of H radical into structure) should be further investigated. Moreover, at the higher BC:W ratio (Misc 700-6 and Misc 700-7) and longer sonication, the organics loss (C content) is lower. It is possible that fixation becomes an important process here, compensating for some of the extractive loss. These processes, along with mineral leaching, lead to increase in heating value, (see Tables 2 and 4). When the stoichiometric ratio was further increased to 30, 40 or 80 g biochar in 250 ml of H₂O (Misc 700-8 to Misc 700-12), the observed synergisms in mineral leaching declined. A likely reason for this decline is that the solutions became more basic. which retarded the dissolution of metallic ions. Moreover, relatively larger biochar particles of 75–250 µm (with majority of the particles in the higher size range, 106-250 µm) were used for runs Misc 700-9 through Misc 700-12. It is known that microparticles in a liquid under ultrasound irradiation play the role of cavitation nuclei, and the number of cavitation bubbles increases with heterogeneous nucleation [27]. However, suspension of hydrophobic microparticles in liquid stabilizes the cavitation bubbles, which are known as armoured bubbles. Hence, bubble oscillation and collapse are constrained, which may lower the cavitation intensity [28-30]. If biochar supplies a source of such hydrophobic microparticles, increasing the load of BC could decrease the effectiveness of cavitation. Along with higher pH, it may be that mass transfer limitations significantly retard the mineral leaching for these runs with particles of higher size range. As stated in the Experimental Section, the run with 80 g biochar (Misc 700-8) had an obvious mixing problem; cavitation took place in only a small region around the tip of ultrasound horn, and the low result for mineral leaching should be considered anomalous.

Biochar serves as a remarkable substrate for the above observed synergisms of the single-stage treatment process.

3.3.3. Implications of mineral and ultimate analyses

As stated earlier, Si inhibits the gasification rate, and Na and K cause fouling and slagging in gasification [1]. Note that K is a soil nutrient. Table 5 shows the benefit of employing $\rm CO_2$ bubbling to the increased leaching of Na, Si, and K from biochar compared to He bubbling (from 18 to 44%, 16 to 29%, and 45 to 62%, respectively). Misc 700-6 and Misc 700-7 had the highest extent of extraction of all of the above minerals, suggesting the significant roles of BC-to-water ratio when ultrasound is employed. As stated in the last section, the observed increase in mineral extraction for runs Misc 700-3 through Misc 700-7 with increasing BC-to-water ratio is likely contributed by the increasing amount of $\rm CO_2$ absorbed by the solution during bubbling.

Large biochar particles were used in Runs Misc 700-9 through Misc 700-12. The observed lower extraction efficiency for those runs can be attributed in part to mass transfer limitations.

Although the presence of CO_2 in the solution benefits mineral dissolution, carbon fixation, and higher heating values, the effects of varying CO_2 concentration in the headspace (7 and 15% CO_2 , Misc 700-6 and Misc 700-7, respectively) during sonication shown in Table 5 seems insignificant. This observation is similar to those of switchgrass BC shown in Table 2. At the outset of this study, CO_2 concentration in the headspace was considered a possible variable due to its impacts on mineral leaching and sonolysis reactions. Moreover, since typical flue gas from coal-fired power plant has 15% CO_2 , these experiments were designed with the hope to achieve the synergism by passing flue gas over a biochar/water solution – without the expensive CO_2 capture for the bubbling process in practice.

The most striking data in Table 6 are the high gains in hydrogen when the biochar-to-water ratio was 15 g to 250 ml (Misc 700-6 and Misc 700-7). The hydrogen gains in BC were 43 and 38% for these two runs, respectively, which were much higher than those of BCs treated under other conditions. Moreover, biochars from these two runs exhibited the highest mineral leaching. It should be noted that the H

Table 6 Changes in elemental composition and heating values of miscanthus biochar.

		*	*	*	*	o*					
	Ash*	C*	H [*]	N*	O [*]	S*	Overall Weight Change, % [*]	Atomic C/O ratio [*]	Atomic H/O ratio*	Heating Value, kcal/g [*]	Energy gained/Energy consumed [*]
Raw Misc 700-a, wt%	6.23	85.22	1.32	0.32	6.85	0.04	Gittinge, 70	16.59	3.08	7.15	consumed
Misc 700-1	5.51	85.94	1.40	0.32	6.80	0.02		16.85	3.29	7.18	
Change during treatment, %	-13%	-0.77%	4.36%	-1.6%	-2.3%	-51%	-1.6%	1.6%	6.8%	0.44%	
Misc 700-2	4.88	86.62	1.35	0.32	6.66	0.04		17.34	3.24	7.27	
Change during treatment, %	- 24%	-0.73%	-0.11%	-2.3%	-5.0%	-2.3%	-2.3%	4.5%	5.2%	1.7%	
Misc 700-3	4.86	86.73	1.33	0.33	6.16	0.04		18.77	3.45	7.33	0.707
Change during treatment, %	- 25%	-1.7%	-2.70%	-0.41%	-13%	-3.4%	-3.4%	13%	12%	2.5%	
Misc 700-4	4.72	86.77	1.33	0.32	6.87	0.03		16.84	3.10	7.31	0.946
Change during treatment,	-27%	-1.9%	-2.93%	-3.7%	-3.4%	- 28%	-3.7%	1.5%	0.46%	2.2%	
Misc 700-5	4.96	86.91	1.33	0.31	6.48	0.02		17.88	3.28	7.29	0.899
Change during treatment, %	-23%	-0.93%	-2.12%	-5.9%	-8.1%	-51%	-2.9%	7.8%	6.5%	2.0%	
Misc 700-6	4.27	86.75	1.93	0.26	6.93	0.02		16.69	4.46	7.48	10.0
Change during treatment, %	-33%	-0.66%	42.7%	-21%	-1.3%	-51%	-2.4%	0.62%	45%	4.6%	
Misc 700-7	4.21	86.74	1.87	0.27	6.94	0.02		16.66	4.31	7.45	8.98
Change during treatment, %	-34%	-0.62%	38.3%	-18%	-1.1%	-51%	-2.4%	0.46%	40%	4.2%	
Misc 700-8	5.24	77.96	1.33	0.32	14.54	0.04		7.15	1.46	6.71	-73.4
Change during treatment, %	-17%	-9.46%	-0.28%	-1.0%	110%	-1.0%	-1.0%	-57%	-52%	-6.2%	
Raw Misc 700-b, wt%	5.25	84.43	1.72	0.30	7.17	0.03		15.70	3.84	7.42	
Misc 700-9	4.69	84.95	1.75	0.28	7.42	0.02		15.27	3.77	7.45	2.04
Change during treatment, %	-12%	-1.4%	-0.26%	-8.5%	1.4%	- 35%	-2.0%	-2.8%	-1.7%	0.44%	
Misc 700-10	4.69	85.09	1.77	0.29	7.38	0.02		15.37	3.84	7.50	4.68
Change during treatment, %	-12%	-1.2%	0.84%	-5.3%	0.86%	- 35%	-2.0%	-2.1%	-0.02%	1.0%	
Misc 700-11**	4.74 (± 0.02)	84.60 (± 0.11)	1.79 (± 0.03)	$0.29 (\pm 0.00)$	7.64 (± 0.18)	$0.03 (\pm 0.01)$		14.76 (± 0.32)	$3.75 (\pm 0.06)$	$7.44 (\pm 0.01)$	1.64 (± 0.28)
Change during treatment, %	-11%	-1.1%	2.74%	-4.6%	5.2%	-1.3%	-1.3%	-6.0%	-2.3%	0.27%	
Misc 700-12	4.79	84.80	1.78	0.29	7.21	0.02		15.68	3.95	7.48	5.16
Change during treatment, %	- 9.7%	-0.63%	2.39%	-4.4%	-0.51%	- 34%	-1.1%	-0.12%	2.9%	0.86%	

^{*} Analyses done based on dried weight.
** Analyses done in duplicate with the standard deviations reported.

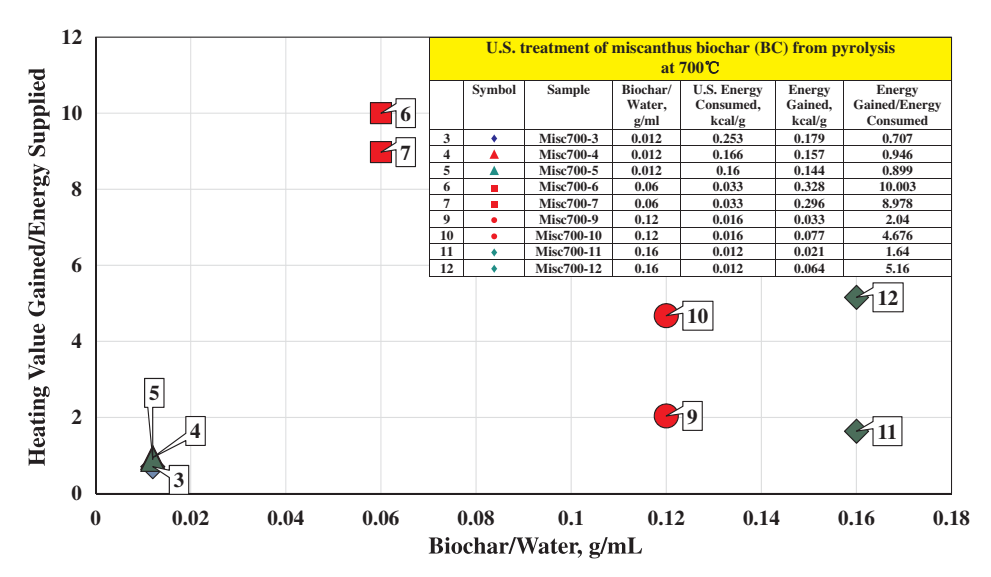


Fig. 5. Changes in the ratio of HVG/ES of miscanthus BC using the ultrasound horn. For processes driven by cavitation, the presence and amount of solids can have significant bearing on the experimental results. This is also observed in the US treatment of miscanthus BC at varying US intensity and BC weight. The heating value gains of the BC in relation to the US energy supplied increased as the BC:H₂O ratio was increased from 0.012 to 0.06 g/ml, but then decreased when the system became too viscous at ratios 0.120 and 0.160. The US treatment with 15 g of BC and 250 ml of $\rm CO_2$ -saturated DI water gave the best result.

content from the elemental analysis is the H associated with organics only. We observed O reduction during treatment. Therefore, the increase in %H is not a simply the result of physical or chemical hydration. Although all the treatments resulted in net carbon loss on a weight-adjusted basis, the amount of loss in %C values varied from 0.53 to 1.63, depending on the treatment. Runs 700-6 and 700-7 showed the least amount of loss. One explanation is that carbon loss from organic leaching was partly offset by carbon fixation from CO_2 . At the same time, the changes in oxygen content were remarkably low for Misc 700-6 and 700-7. These combined processes result in a remarkably high gain in the BC's higher heating values, (see Table 4 and Fig. 5).

Fig. 5 illustrates the effect of BC-to-water ratio on the ratio of biochar's heating value gain to the amount of ultrasound energy supplied, or HVG/ES. HVG/ES increased from approximately 1 to 10 when the BC/H₂O ratio increased from 0.012 to 0.06 g/ml, followed by a decline at higher BC/H₂O ratios. The value HVG/ES ~ 10 for Misc 700-6 shows that the ultrasound treatment is an efficient technique for concentrating energy in BC. It should also be noted that, though the heating value of biochar demonstrated a significant increase after ultrasound treatment in presence of CO₂, the total heat content in most cases (except Misc 700-6 and Misc 700-7) slightly (with the average of 0.12 kcal/g) reduced mainly due to the mineral leaching and its subsequent effect on biochar final weight. However, total heat content of Misc 700-6 and Misc 700-7 increased by 0.15 and 0.12 kcal/g which might be due to the remarkable increase in H content and small loss of C content of these samples.

Several factors may contribute to the initial increase in HVG/ES with increasing BC/water stoichiometric ratio. As discussed earlier, a larger amount of biochar implies a larger reservoir for CO₂ absorption during bubbling. Higher CO₂ enhances mineral leaching and carbon fixation during sonication. Moreover, gas entrapped in the microscopic crevices or pores on the rough biochar surface can serve as cavitation initiation sites. These gaseous nuclei expand and contract with alternating cycles of rarefactions and compressions, releasing bubbles into the mixture that participate in and enhance cavitation reactions during bubble collapse, or implosion [31]. Therefore, an increase in the biochar-to-water ratio suggests an increase in the available cavitation initiation sites, thereby improving the utilization of ultrasound energy.

At higher stoichiometric BC/water ratios of 0.12, 0.16 and 0.20, the decline in HVG/ES shown in Fig. 5 can be associated with several factors. First, as stated earlier, the larger particles used in these experiments are likely to limit the mass transfer of reactants and products in the fluid. Second, there is likely a weakening of acoustic energy throughout the system, resulting in significant reduction in the active region of cavitation and limited or imperfect mixing [32]. The BC/ $\rm H_2O/$

 ${\rm CO_2}$ systems with higher BC loading were noticeably not as fluid and bubbly as those at lower stoichiometric ratios. For example, at a BC/ ${\rm H_2O}$ of 0.20 g/ml, the mixing effect due to the ultrasonic streaming was visibly localized within a small region around the tip area of the transducer, indicating that the acoustic energy does not reach into the bulk of the mixture to create sonochemical or mixing effects. Third, water is a source of hydrogen, and the extent of hydrogenation of biochar is expected to be lowered as the proportion of water decreases.

In the present study, the optimal BC/water ratio for the acoustic treatment of miscanthus BC under ambient conditions was 0.06 g/ml. The existence of optimal BC-to-water ratios in ultrasound-assisted treatments of biomass have also been reported. For example, Velmurugan and Muthukumar [33] reported an optimal value of 0.05 g/ml in the sono-assisted pretreatment and hydrolysis of raw and pretreated sugar cane bagasse. Similarly, Sasmal et al. [34], in a study of ultrasound-assisted lime pretreatment of biomasses toward bioethanol production, reported that the BC-to-water ratio was crucial to achieve optimal results for moj (Albiza lucida) biomass.

3.3.4. Sonolysis of CO2 in water with and without biochar

The observations stated, represent a remarkably attractive route of carbon chemical looping for recycling, reusing and reducing CO2 from combustion sources that has been considered a grand challenge. CO2 is the only carbon source external to biochar in the treatment. It is therefore reasonable to assume that the observed carbon fixation starts with C1 chemistry of CO₂. Moreover, since ultrasound plays a pivotal role in the complex 3-phase biochar/H₂O/CO₂ system, it is plausible to hypothesize two sequential groups of reactions for the observed C fixation: sonolysis of CO2 followed by reactions between the sonolysis products and biochar. Several have studied the sonolysis of CO2 in aqueous solution [32,35,36]. Henglein et al. revealed that CO₂ plays two major roles: scavenging hydrogen radicals and decomposition to CO [36]. It is known that ultrasound splits water to form hydrogen and hydroxyl radicals (R2). When CO2 is absent, two similar radicals can combine to form H2 (R3) and H2O2 (R4); the reverse reaction of R1 also takes place.

$$H$$
— OH \longrightarrow $H \cdot + \cdot OH$ (R2)

$$H \cdot + \cdot H \longrightarrow H - H$$
 (R3)

$$HO \cdot + \cdot OH \longrightarrow HO - OH$$
 (R4)

When CO_2 is present, however, it scavenges •H from the sonolysis of water to form •COOH (R5). Small amounts of formic acid (HCOOH) are also observed, which could be explained by radical recombination (R6).

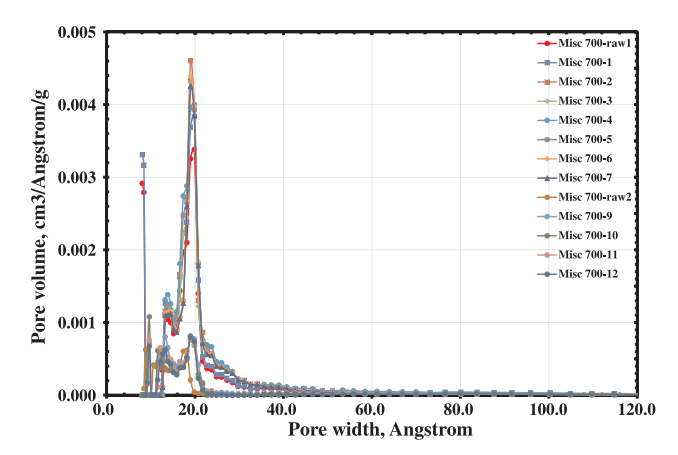


Fig. 6. Pore size distribution for N_2 at 77 K on miscanthus BC using the NLDFT equilibrium model (slit-pore).

$$O=C=O + \cdot H \longrightarrow O=C-O-H$$
 (R5)

$$O = C - O - H + \cdot H \longrightarrow O = C - O - H$$

$$H$$
(R6)

The •COOH formed by (R5) can also fragment to CO and •OH (R7). [37] Since CO was a major product of sonolysis, Henglein postulated that ultrasound also splits CO_2 directly (R8). This dissociation is feasible at a disintegration temperature of 3600 K in a plasma [38], which is a reasonable temperature during sonochemical cavitation collapse [39,40].

$$O=C-O-H$$
 $\longrightarrow O=C: + O-H$ (R7)

$$\vdots O = C = O : + \bullet O \bullet$$
 (R8)

In terms of chemical changes to the biochar, the most striking finding in our results is the increase in %H of about 40% for Misc 700-6 and Misc 700-7, an increase that appears to be beyond the limits of experimental uncertainty. It is possible that hydrogen is adding to C–C π bonds in the biochar, perhaps by sequential reaction with hydrogen atoms as shown in (R13). It is also possible that molecular $\rm H_2$ could reduce π bonds, with the high temperatures of cavitation obviating the normal requirement for a Group 10 metal catalyst. For additions of hydrogen by either route, we would expect the H/O atomic ratio in the system to increase, because no oxygen would be added at the same time (as would happen with the addition of $\rm H_2O$). Table 6 shows generally small changes in H/O, except for Misc 700-6 and Misc 700-7, which show large increases, consistent with the fixing of hydrogen onto bichar. Such fixation would constitute the conversion of ultrasonic energy to chemical energy in the biochar.

$$C = C \qquad \xrightarrow{+ \cdot H} \qquad C - C - H \qquad \xrightarrow{+ \cdot H} \qquad H - C - C - H \qquad (R13)$$

The mechanisms above suggest that CO, formic acid, formaldehyde and H_2 could be involved in modifying the biochar. We remain interested in the possible fixation of carbon from CO_2 to the biochar. Since an early sonochemical reaction is the addition of H^{\bullet} to CO_2 to form a carbon-centered ${}^{\bullet}COOH$ radical (R5), it is possible that the radical adds to a biochar π bond, and the resulting radical combines with another radical, giving a carboxylic acid (R14). Alternatively, as stated above, formic acid is reduced to formaldehyde under sonication (R12). It is known that formaldehyde participates in electrophilic aromatic substitution reactions with aromatic compounds, resulting in hydroxymethylated derivatives (R15). The high temperatures of cavitation might replace the normal requirement for a Lewis acid catalyst for this electrophilic substitution.

$$C = C + O = C - O - H \longrightarrow C - C - C \xrightarrow{O} + \cdot H \longrightarrow H - C - C - C \xrightarrow{O} O - H$$

$$C = C \xrightarrow{H} + H - Ar \longrightarrow HO - CH_2 - Ar$$

$$R14$$

The diradical $\bullet O \bullet$ atom formed in (R8) is very reactive. It could combine with two $\bullet H$ to form H_2O or with another $\bullet O \bullet$ to form O_2 ; it could also react with CO_2 to form more CO and molecular oxygen (R9), or with CO to form O_2 and a carbon atom (R10).

$$\vdots O = C = O \vdots + \bullet O \bullet \longrightarrow \vdots O = C : + : O - O :$$
 (R9)

$$: C = O : + O \cdot \longrightarrow C : + : O - O :$$
 (R10)

Harada systematically investigated the parameters governing the sonochemical reduction of aqueous CO_2 to CO [41]. H_2 and a small amount of O_2 are also products of the process; H_2 generation only becomes large after CO_2 is depleted. More recently, Navarro et al. studied the sonolysis of formic acid, and found that, at high sonication frequency, sonochemically driven reduction of CO leads to the formation of a small amount of formaldehyde as byproduct of HCOOH degradation, possibly via the sequence of (R11), (R7), and (R12). Further reduction leads to smaller amounts of CH_4 , a transformation reminiscent of the Fischer-Tropsch process [42].

The carboxylation sequence (R14) has a consequence: since two new atoms of O would accompany each new atom of C, the C/O ratio would decrease. However, Table 6 shows that this ratio increases for runs Misc 700-1 through Misc 700-7. The ratio does decrease a few % for the larger-particle runs of Misc 700-9 through Misc 700-12. The C/O ratio would stay roughly the same for hydroxymethylation. There is, however, another way to fix carbon that does not involve oxygen. If carbon atoms are created during sonication of CO₂ as shown in (R10), they could conceivably attack biochar π systems as in (R13) and (R14), thereby adding fixed carbon to the biochar framework. It is also conceivable that, during the intense conditions of sonolysis, CO could reduce BC by extracting oxygen atoms from the structure, thereby increasing the C/O ratio. For example, Misc 700-3 and Misc 700-5, using 100% ultrasound amplitude, showed losses of about 10% of their oxygen compositions. The rates of these reactions are difficult to study; in some cases, the proposed mechanism steps are speculative. For the purposes of the discussion here, a qualitative appreciation of likely energetics should be sufficient. As a rule of thumb, the steps that generate radicals will be endergonic with activation energies comparable to the bond dissociation energy of the cleaving bond; steps that combine radicals will be exergonic with near-zero activation energies; and steps where radicals beget other radicals will have moderate energy changes. A recent estimate of activation energy for R2 during sonolysis is $118 \, \text{kcal/mole}$ [43]. This is certainly a feasible E_a in the extreme

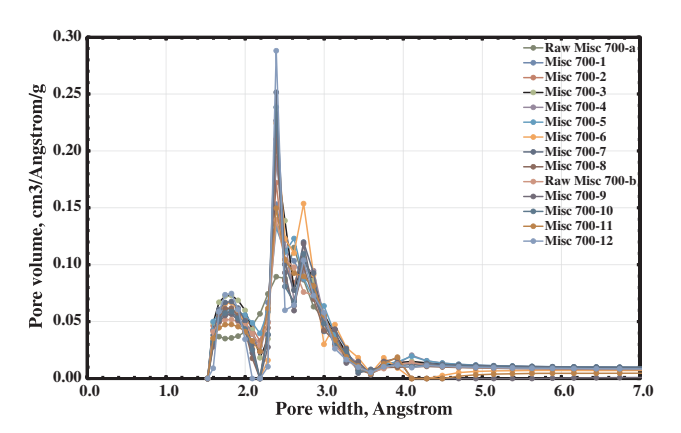


Fig. 7. . Pore size distribution for ${\rm CO_2}$ at 273 K on miscanthus BC using the NLDFT model.

temperature of a collapsing cavitation bubble.

3.3.5. Energy balance

Table 4 shows that the heating values of smaller-particle BCs improve with the application of ultrasound. It has been reported that size and shape of particles (as cavitation nuclei) affect the cavitation. Cavitation preferentially occurs at the surface of small particles due to a lower energy barrier [44]. Table 4 and Fig. 6 show how the gain in HV compares to the amount of ultrasonic energy supplied (HVG/ES). It is clear that under the best conditions; considerably more additional energy can be extracted from a given mass of BC than was expended in activating it. This normally means that ultrasound acted by concentrating BC's existing energy, rather than converting ultrasonic energy into chemical energy. Also in Table 4, the Heat Content Change tracks the actual heat of combustion contained in an entire sample, before and after treatment. Since some organics are removed by leaching, one would expect this heat content to decrease. Indeed this is the case, except for Misc 700-6 and Misc 700-7, where there is a small but distinct increase. This increase is consistent with the chemical hydrogenation suggested above, indicating a transfer of ultrasonic energy to the BC.

This cannot be the entire story, however, because the increase in chemical energy is several times the amount of the ultrasonic energy supplied. It is worth considering another, physical mechanism for at least some of the effects of ultrasound. If there are sequestered pockets of organics in the BC matrix that are not accessed during analytical combustion, sonication could open the BC framework so that they can then combust. This would increase the heat of combustion following treatment. Testing this possibility will require a carbon analytical method other than combustion.

3.3.6. Changes in surface area and pore volume

Table 3 presents the micropore surface area, micropore volume, mesopore surface area and mesopore volume of raw and treated miscanthus BCs. Ultrasound treatment (with dissolved CO2) led to increases in all pore characteristics when the BC-to-water ratio was lower than its optimal value. All treatments remarkably enhanced micropore surface area and micropore volume. However, the level of increase was higher for Misc samples, which were synthesized under higher temperatures, compared with SG samples. Among the Misc samples, Misc700-1 (activated in water free of CO₂) represented a higher enhancement in macroporosity at the cost of lower enhancement in microporosity. The opposite trend was observed in Misc700-2, which was activated under the similar condition, but in water saturated with CO₂. A similar trend was observed in the activation of Raw Misc 700-a and Raw Misc 700-b. The average of the increment in microporosity in Raw Misc 700-a samples (3, 4, 5, 6), which were activated under open air, was higher than the increment for Misc 700-b samples (9, 10, 11, 12),

which were activated under higher CO_2 concentrations (7 and 15%). Indeed, the effect of the BC-to-water ratio on these pore characteristics followed the same trend as that of heat values. Misc 700-6 and Misc 700-7 had the highest increases in the pore properties. Moreover, Misc 700-10 and Misc 700-12, treated with 7% CO_2 in the headspace, showed higher DR- CO_2 surface areas than Misc 700-9 and Misc 700-11, treated with 15% CO_2 in the headspace. As discussed earlier, treatment of switchgrass BC followed a similar trend as miscanthus BC. SG 550-4 treated under 1 atm atmosphere of CO_2 showed lower micropore surface area than SG 550-2 treated in the open air.

Figs. 6 and 7 illustrate that the BCs possess mesopores and micropores. The DFT *micropore* size distribution shown in Figs. 3 and 7 suggests that both switchgrass and miscanthus BCs have micropores within a narrow range of $1.5-3.5\,\text{Å}$. The raw BC with smaller particle size (Misc 700-a) had a more developed mesopore size distribution than did raw BC of larger particles (Misc 700-b). The results suggest that BCs of smaller particle size are more amenable to the treatment. Similar to switchgrass BC, treatments of miscanthus BC led to a sharp increase in micropores of $2.4\,\text{Å}$.

3.3.7. Effect of acoustic intensity

Acoustic intensity is a measure of the rate and concentration of energy delivered to a system and it is directly related to the amplitude of vibration of the radiating face of the horn. An increase in the amplitude of the ultrasonic wave results in an increase in cavitation intensity [31]. Generally, sonochemical efficiency increases with the intensity of the acoustic field, but for a single-frequency operation, there is a system-specific optimum beyond which a decline in yield is observed [45]. Xie et al. [46] investigated the efficiency of biological phosphorus removal using low intensity ultrasound and reported the existence of an optimum acoustic intensity of 0.2 W/cm². Saez et al. [47] also reported the existence of an optimum acoustic intensity in their study of the characterization of a 20 kHz sonoreactor. In the range of 0-8 W/cm², they found an optimal value of 2.8 W/cm². In the current study, two different amplitude settings, 5% and 100%, were used, with the total energy output being held constant by adjusting the duration of irradiation. Mineral matter removal and heating value gains tended to be slightly greater at lower than higher acoustic intensity. There are two possible reasons for this. First, the better results with low intensity ultrasound could be a result of longer contact time between biochar and the water saturated with CO2 at low ultrasound power. The treatment process involves a complex reaction network, and the rate

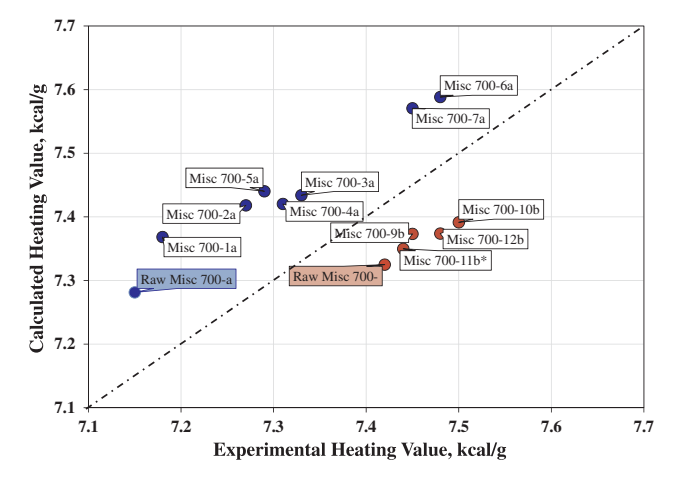


Fig. 8. Comparison of experimentally observed higher heating values with those predicted by the empirical equation of Channiwala and Parikh (2002): Higher Heating Value = (0.3491 $\rm X_C + 1.1783~X_H + 0.1005~X_S - 0.0151~X_N - 0.1034~X_O - 0.0211X_{ash})\,MJ/kg$. The formula gave a maximal error of 2.62% and an average error of 1.61%. **●**: Particle size ranges of 75–106 μm **●**: Particle size ranges of 75–250 μm.

and intensity of sonolysis reactions can be different under low-power, long-time irradiation as compared to those under a high-power, short-time process. For instance, our original observation of the benefits of biochar treatment [1] was conducted with lower power over longer times, and with high $\rm CO_2$ concentration in the headspace. Second, it could be the result of bubble cloud formation around the tip of the horn when high cavitation intensity is present. These bubble clouds attenuate sound waves traveling through the system, thereby resulting in decreased energy transfer efficiency to the reaction medium, which has been called the decoupling effect [48].

Since the maximum size, number, and lifetime of bubbles before collapse in a sonochemical reaction is a system-specific and complex function of different parameters including acoustic intensity [49], there might be an optimum amplitude setting between 5 and 100% with which the best results can be obtained. The effectiveness of sonication in terms of power parameters is a function of cavitation activity, and not necessarily the total power applied to the system.

3.3.8. Prediction of higher heating value (HHV) based ultimate analysis

We compared the measured higher heating values (HHV) of raw and treated miscanthus biochar samples with the empirical formula of Channiwala and Parikh [50], which is based on ultimate analysis, where X = the experimental % weight fraction of each component:

$$\begin{split} HHV &= (0.3491\,X_C + 1.1783\,X_H + 0.1005\,X_S - 0.0151\,X_N - 0.1034\,X_O \\ &- 0.0211\,X_{ash})\,MJ/kg. \end{split}$$

The comparison shown in Fig. 8 suggests that the estimation based on this formula is reasonably accurate with maximal and average errors of about 2.62% and 1.61%, respectively. Hydrogen and carbon play the most important roles in contributing to heating value, as per their large coefficients. Hydrogen content in the aforementioned equation has the largest coefficient suggesting the distinct impact of H fixation on the gain in HHV. The extraordinarily high H contents of Misc 700-6a and Misc 700-7a support the important role of H fixation. On the other hand, the best correlation among BCs treated with $\rm CO_2$ was with %C. The six samples with HHV > 7.4 kcal/g all had %C > 86%, while the five samples with HHV < 7.4 kcal/g all had %C < 86%. This correlation is suggestive of a role for C fixation in the observed heating value gains. However, comparing the coefficient of $\rm X_H$ with that of $\rm X_C$, demonstrates that the change of H content must play a more prominent role in HHV.

4. Conclusions

Ultrasonic pretreatment of biochar in water with dissolved CO_2 can be an economic route to the improvement of a gasifier's performance in several aspects. However, the pretreatment process is rather complex, as it is governed by a wide range of variables associated with feedstock, pyrolysis and treatment per se. This study examines the feasibility of the concept and the parameters that affects the benefits of pretreatment. The emphasis is placed on the enhancement in biochar heating value and other related properties in the early stage of the treatment process.

The ratio of biochar's Heating Value Gain to the ultrasound Energy Supplied (HVG/ES) increased to about 10 when the biochar-to-water ratio was increased from 0.012 to 0.06 g/ml. Further increases in the stoichiometric ratio caused HVG/ES to decline. The large HVG/ES value at the optimal condition suggests the feasibility of the treatment concept.

The CO_2 concentration in the reactor plays an important role during the treatment, affecting pH and cavitation. The BC-water- CO_2 ratio has a profound impact on the hydrogen and carbon gains of biochar, as water and CO_2 are the only H and C sources in the reacting system, respectively. Biochar particle size and ultrasound power affect the mass transfer and cavitation properties in the three-phase system. Mineral

leaching, an important contributor to biochar energy gain, is affected by pH, CO₂ concentration, extracted organic species, and mass transfer limitations.

The results of the current study are consistent with the findings that sonolysis of aqueous CO_2 forms H_2 , CO, formic acid and formaldehyde. It is possible that these products of sonolysis contribute to the observed chemical changes of biochar. Gain in biochar's HHV correlates well to the ultimate analysis. The correlation also suggests that hydrogen fixation distinctively contributes to the gain in HHV. Carbon fixation is also a contributor.

A thorough exploration of the three-phase treatment system is far from complete, but further study is warranted by these results.

Acknowledgment

This project is supported by the National Science Foundation of the United States (NSF EPSCoR RII Grant No. OIA-1632899), to whom the authors are grateful.

References

- Chen W-Y, Mattern DL, Okinedo E, Senter JC, Mattei AA, Redwine CW. Photochemical and acoustic interactions of biochar with CO₂ and H₂O: Applications in power generation and CO₂ capture. AIChE J 2014;60(3):1054–65.
- [2] Chatterjee R, Sajjadi B, Mattern DL, Chen W-Y, Zubatiuk T, Leszczynska D, et al. Ultrasound cavitation intensified amine functionalization: a feasible strategy for enhancing CO2 capture capacity of biochar. Fuel 2018;225:287–98.
- [3] Sajjadi B, Chen WY, Broome JW, Mattern DL, Egiebor N, Hammer NI, et al. Urea functionalization of ultrasound-treated biochar: a feasible strategy for enhancing heavy metal adsorption capacity. Ultrason-Sonochem 2018; Under minor revisions.
- [4] Wall TF, Liu G-s Wu, H-w Roberts DG, Benfell KE, Gupta S, et al. The effects of pressure on coal reactions during pulverised coal combustion and gasification. Prog Energy Combust Sci 2002;28(5):405–33.
- [5] Tennant JB. Gasification systems overview, National Energy Technology Laboratory. https://www.netl.doe.gov/File%20Library/Research/Coal/energy%20systems/gasification/doe-gasification-program-overview.pdf [accessed 05.06.2018].
- [6] Klüpfel L, Keiluweit M, Kleber M, Sander M. Redox properties of plant biomass-derived black carbon (biochar). Environ Sci Technol 2014;48(10):5601–11.
- [7] Linsen G. Physical and chemical aspects of adsorbents and catalyst (Chapter 9). London: Academic Press; 1970.
- [8] Mattson JS, Mark HB. Activated carbon: surface chemistry and adsorption from solution. In: M. Dekker, ed. New York; 1971.
- [9] Budai A, Wang L, Gronli M, Strand LT, Antal MJ, Abiven S, et al. Surface properties and chemical composition of corncob and miscanthus biochars: effects of production temperature and method. J Agric Food Chem 2014;62(17):3791–9.
- [10] Weber K, Quicker P. Properties of biochar. Fuel 2018;217:240–61.
- [11] Chintala R, Mollinedo J, Schumacher TE, Malo DD, Julson JL. Effect of biochar on chemical properties of acidic soil. Arch Agron Soil Sci 2014;60(3):393–404.
- [12] Corapcioglu MO, Huang CP. The surface acidity and characterization of some commercial activated carbons. Carbon 1987;25(4):569–78.
- [13] Sajjadi B, Chen WY, Egiebor N. Physical activation of biochar for energy and environmental applications; a comprehensive literature review. Rev Chem Eng 2018. https://doi.org/10.1515/revce-2017-0113. in press.
- [14] Sajjadi B, Zubatiuk T, Leszczynska D, Leszczynski J, Chen WY. Chemical activation of biochar for energy and environmental applications; a comprehensive literature review. Rev Chem Eng 2018. https://doi.org/10.1515/revce-2018-0003. in press.
- [15] Gathitu BB, Chen W-Y, McClure M. Effects of coal interaction with supercritical CO₂: physical structure. Ind Eng Chem Res 2009;48(10):5024–34.
- [16] Cha JS, Park SH, Jung S-C, Ryu C, Jeon J-K, Shin M-C, et al. Production and utilization of biochar: a review. J Ind Eng Chem 2016;40:1–15.
- [17] Thines KR, Abdullah EC, Mubarak NM, Ruthiraan M. In-situ polymerization of magnetic biochar – polypyrrole composite: a novel application in supercapacitor. Biomass Bioenergy 2017;98:95–111.
- [18] Lievens C, Mourant D, Hu X, Wang Y, Wu L, Rossiter A, et al. A case study: what is leached from mallee biochars as a function of pH? Environ Monit Assess 2018;190(5):294.
- [19] Silber A, Levkovitch I, Graber ER. pH-dependent mineral release and surface properties of cornstraw biochar: agronomic implications. Environ Sci Technol 2010;44(24):9318–23.
- [20] Wu H, Yip K, Kong Z, Li C-Z, Liu D, Yu Y, et al. Removal and recycling of inherent inorganic nutrient species in mallee biomass and derived biochars by water leaching. Ind Eng Chem Res 2011;50(21):12143–51.
- [21] Bussemaker MJ, Zhang D. Effect of ultrasound on lignocellulosic biomass as a pretreatment for biorefinery and biofuel applications. Ind Eng Chem Res 2013;52(10):3563–80.
- [22] Technology HU. Ultrasonic degassing and defoaming of liquids. https://www.hielscher.com/degassing_01.htm [accessed 13.04.2018].
- [23] Thommes M, Kaneko K, Neimark AV, Olivier JP, Rodriguez-Reinoso F, Rouquerol J, et al. Physisorption of gases, with special reference to the evaluation of surface area and pore size distribution (IUPAC Technical Report). Pure Appl Chem 2015;87(9–10):1051–69.
- [24] Particle sciences. An overview of the zeta potential. Part Sci 2012;2(1-4).
- [25] Yuan J-H, Xu R-K, Zhang H. The forms of alkalis in the biochar produced from crop residues at different temperatures. Bioresour Technol 2011;102(3):3488–97.
- [26] Park K-H, Lee C-H, Ryu S-K, Yang X. Zeta-potentials of oxygen and nitrogen enriched activated carbons for removal of copper ion. Carbon Lett 2007;8(4):321–5.

- [27] Bremond N, Arora M, Ohl C-D, Lohse D. Controlled multibubble surface cavitation. Phys Rev Lett 2006;96(22):224501.
- [28] Stocco A, Drenckhan W, Rio E, Langevin D, Binks BP. Particle-stabilised foams: an interfacial study. Soft Matter 2009;5(11):2215–22.
- [29] Chen H, Li J, Zhou W, Pelan EG, Stoyanov SD, Arnaudov LN, et al. Sonication-micro-fluidics for fabrication of nanoparticle-stabilized microbubbles. Langmuir 2014;30(15):4262–6.
- [30] Ge H, Li J, Chen HS. Influence of microparticle size on cavitation noise during ultrasonic vibration. AIP Adv 2015;5(9):097145.
- [31] Mason TJ, Peters D. Practical sonochemistry: power ultrasound uses and applications. Elsevier Science; 2002.
- [32] Shah YT, Pandit AB, Moholkar VS. Cavitatin reaction engineering. New York: Kluwer
- Academic/Plenum Publishers; 1999.
 [33] Velmurugan R, Muthukumar K. Utilization of sugarcane bagasse for bioethanol produc-
- tion: sono-assisted acid hydrolysis approach. Bioresour Technol 2011;102(14):7119–23.

 [34] Sasmal S, Goud VV, Mohanty K. Ultrasound assisted lime pretreatment of lignocellulosic biomass toward bioethanol production. Energy Fuels 2012;26(6):3777–84.
- [35] Rooze J. Cavitation in gas-saturated liquids. Chemical Engineering and Chemistry Department. Ph.D. Eindhoven, Netherlands: Eindhoven University of Technology; 2012.
- [36] Henglein A. Sonolysis of carbon dioxide, nitrous oxide and methane in aqueous solution. Zeitschrift für Naturforschung B 1985;40(1):100-7.
- [37] Harada H, Hosoki C, Ishikane M. Sonophotocatalysis of water in a CO2–Ar atmosphere. J Photochem Photobiol, A 2003;160(1):11–7.
- [38] Kwak HS, Uhm HS, Hong YC, Choi EH. Disintegration of carbon dioxide molecules in a microwave plasma torch. Sci Rep 2015;5:18436.
- [39] Margulis MA. Fundamental problems of sonochemistry and cavitation. Ultrason

- Sonochem 1994;1(2):S87-90.
- [40] Suslick KS, Hammerton DA, Cline RE. Sonochemical hot spot. J Am Chem Soc 1986;108(18):5641–2
- [41] Harada H. Sonochemical reduction of carbon dioxide. Ultrason Sonochem
- [42] Navarro NM, Chave T, Pochon P, Bisel I, Nikitenko SI. Effect of ultrasonic frequency on the mechanism of formic acid sonolysis. J Phys Chem B 2011;115(9):2024–9.
- [43] Merouani S, Hamdaoui O, Rezgui Y, Guemini M. Mechanism of the sonochemical production of hydrogen. Int J Hydrogen Energy 2015;40(11):4056–64.
- [44] Zhang L, Belova V, Wang H, Dong W, Möhwald H. Controlled cavitation at nano/microparticle surfaces. Chem Mater 2014;26(7):2244–8.
- [45] Sutkar VS, Gogate PR. Design aspects of sonochemical reactors: techniques for understanding cavitational activity distribution and effect of operating parameters. Chem Eng J 2009;155(1):26–36.
- [46] Xie B, Wang L, Liu H. Using low intensity ultrasound to improve the efficiency of biological phosphorus removal. Ultrason Sonochem 2008;15(5):775–81.
- [47] Sáez V, Frías-Ferrer A, Iniesta J, González-García J, Aldaz A, Riera E. Characterization of a 20 kHz sonoreactor. Part II: analysis of chemical effects by classical and electrochemical methods. Ultrason Sonochem 2005;12(1):67–72.
- [48] Sivakumar M, Pandit AB. Ultrasound enhanced degradation of Rhodamine B: optimization with power density. Ultrason Sonochem 2001;8(3):233–40.
- [49] Gogate PR, Sutkar VS, Pandit AB. Sonochemical reactors: important design and scale up considerations with a special emphasis on heterogeneous systems. Chem Eng J 2011;166(3):1066–82.
- [50] Channiwala SA, Parikh PP. A unified correlation for estimating HHV of solid, liquid and gaseous fuels. Fuel 2002;81(8):1051–63.